HEFAT 2014
10th International Conference on Heat Transfer, Fluid Mechanics and Thermodynamics
14 – 16 July 2014
Orlando, Florida

TOWARDS LOW-COST MICROCHANNEL HEAT EXCHANGERS: VEHICLE HEAT RECOVERY VENTILATOR PROTOTYPE

Denkenberger D.[1]* Parisi M.[2] and Pearce J.M.[3]
[1]*Author for correspondence, Denkenberger Inventing and Consulting, Durango, CO, USA, E-mail: david.denkenberger@colorado.edu
[2]Niagara Thermal Products, Niagara Falls, NY, USA
[3]Michigan Technological University, Houghton, MI, USA

ABSTRACT

Vehicles could save ~110 million gallons of gasoline per year in the U.S. with heat exchangers acting as heat recovery ventilators in the air conditioning systems. Even more energy could be saved with in-vehicle heat exchangers by reducing heating energy in plug-in vehicles. Currently, vehicles do not have heat recovery ventilators because of the high cost of conventional metal heat exchangers. To overcome this challenge, low-cost expanded polymer microchannel heat exchangers were studied. Forward conduction laser welding was used to join 25-micron thick linear low-density polyethylene sheets, which were then fixed into shape and expanded. The microchannel polymer heat exchangers were tested at various air flow rates. At the maximum flow rate, the effectiveness was ~70% and the implications of this expanded heat exchanger in other applications are discussed.

INTRODUCTION

Heat exchangers (HXs) transfer heat from one fluid to another (both liquids and gases are considered fluids) and are widely used across a range of conventional industries. Such applications include: refrigeration cycles, heat recovery, industrial processes, vehicles, and conventional power plants [1]. In addition, the renewable energy field has many applications of HXs including: fuel cells, concentrated solar power, solar hot water, compressed air energy storage [2], wind turbines, geothermal, and solar water pasteurization. The latter application has the potential to save the lives of thousands of children a day [3,4].

Polymers are already being used for HXs in corrosive environments, such as industrial applications [1], condensing furnaces [5], and have been proposed for ocean thermal energy conversion [6]. Also, the low cost of polymers are attractive in air-to-air applications, where the thermal resistance in the fluid is high [7]. In high-pressure applications, where the polymer cannot be made as thin, additives such as graphite can increase the thermal conductivity of the polymer [8]. Also, fiber reinforcement increases strength and temperature resistance of polymers, allowing one polymer HX to be designed to withstand a pressure of 60 atmospheres, which is sufficient for refrigerant cycles [1].

One promising approach to the design of HXs is to use microchannels. Microchannel HXs (one definition being hydraulic diameter < 1 mm) have low material cost, weight, and volume, but the current manufacturing techniques used in production are expensive. Commercialized methods of producing microchannel HXs are etching, LIGA (lithography, electroplating and molding), micromachining, and stereolithography [9]. Recent work [10] has provided a low-cost method using laser welding of microchannel HX fabrication for polymer-based HXs.

Following on this development, this paper presents the design, fabrication, and preliminary tests of an air-to-air cross flow prototype. This application is a vehicle heat recovery ventilator (HRV). The results are discussed to guide further technological development of this approach to HX design and fabrication.

NOMENCLATURE

Symbol	Units	Explanation
A	[m^2]	Total area for heat transfer
C	[-]	Heat capacity rate ratio
C_c	[kJ/(s*K)]	Heat capacity rate on cold side
C_h	[kJ/(s*K)]	Heat capacity rate on hot side
C_{min}	[kJ/(s*K)]	Minimum heat capacity rate
C_{max}	[kJ/(s*K)]	Maximum heat capacity rate
C_p	[kJ/(kg*K)]	Specific heat
HX	[-]	Heat exchanger
h	[W/(m^2*K)]	Heat transfer coefficient
$LLDPE$	[-]	Linear low density polyethylene
$\dot{m}$	[kg/s]	Mass flow rate
NTU	[-]	Number of transfer units
Pa	[N/m^2]	Pascal
$\dot{q}$	[kW]	Heat rate
T	[K]	Temperature
Greek		
η	[-]	Effectiveness

SUBSCRIPTS

Symbol	Meaning
C	Cold fluid
H	Hot fluid
I	In
min	Minimum
O	Out

BACKGROUND

The following HX parameter background is based on McQuiston [11]. The performance of a HX is characterized by its effectiveness, η, defined as the actual heat transfer rate as a fraction of the maximum heat transfer rate:

$$\eta = \frac{\dot{q}}{\dot{q}_{max}}, \qquad \textbf{Equation 1}$$

where the actual heat transfer rate is:

$$\dot{q} = C_h(T_{hi} - T_{ho}) = C_c(T_{co} - T_{ci}), \qquad \textbf{Equation 2}$$

where T_{hi} is the temperature of the hot fluid going into the HX, T_{ho} is the temperature of the hot fluid coming out of the HX, T_{ci} is the temperature of the cold fluid going into the HX, and T_{co} is the temperature of the cold fluid coming out of the HX. Also, the hot heat capacity rate is:

$$C_h = \dot{m}_h C_{ph}, \qquad \textbf{Equation 3}$$

where $\dot{m}_h$ is the hot mass flow rate and C_{ph} is the hot specific heat. Furthermore, the cold heat capacity rate is:

$$C_c = \dot{m}_c C_{pc}, \qquad \textbf{Equation 4}$$

where $\dot{m}_h$ is the hot mass flow rate and C_{ph} is the hot specific heat. The maximum heat transfer rate is:

$$\dot{q}_{max} = C_{min}(T_{hi} - T_{ci}), \qquad \textbf{Equation 5}$$

where C_{min} is the minimum of C_h and C_c. For a counter-flow HX,

$$\eta = \frac{1-e^{-NTU(1-C)}}{1-Ce^{-NTU(1-C)}} \qquad \textbf{Equation 6}$$

where C is heat capacity flow ratio = C_{min}/C_{max}; NTU is "number of transfer units:"

$$NTU = \frac{hA}{C_{min}}, \qquad \textbf{Equation 7}$$

where A is the heat transfer area and h is the heat transfer coefficient.

For the rest of this paper, effectiveness will be used in the temperature sense, rather than heat rate:

$$\eta_h = \frac{T_{hi}-T_{ho}}{T_{hi}-T_{ci}}, \qquad \textbf{Equation 7}$$

and

$$\eta_c = \frac{T_{co}-T_{ci}}{T_{hi}-T_{ci}}. \qquad \textbf{Equation 8}$$

The concept of the expanded microchannel heat exchanger (EMHX) is high-precision joining sheets of material and subsequent expansion [10]. The joining pattern can be achieved by laser welding, inkjet printing of adhesives, acoustic welding, and contact welding. The expansion could be achieved by inflation (stretching or non-stretching of the sheets). Alternatively, rigid plates could be affixed to the top and bottom and pulled apart, resulting in stretching of the sheets. Another possibility is perforated plates on the top and bottom with air being drawn through the plates; these plates would be pulled apart with the device getting narrower and the sheets not stretching. A further possibility is gluing the tips of the bristles on brushes to the top and bottom of the EMHX; these brushes would be pulled apart with the device getting narrower and the sheets not stretching. The materials could be polymers, composites, metals, or ceramic precursors. Mass production, for instance with a roll-to-roll process, could enable low cost [12]. Low cost would enable high surface area and/or multiple stages to produce high effectiveness. Low pressure drop can be achieved with lower velocity and many parallel paths, especially for laminar flow.

FABRICATION

25 µm thick black sheets of linear low-density polyethylene (LLDPE) were used as the material for the vehicle HRV prototypes because it can withstand the maximum temperatures in the engine compartment away from the engine (about 100°C). Also, it has a wide laser welding range, meaning the difference between the decomposition temperature and the melting temperature is a large fraction of the difference between the decomposition temperature and ambient temperature. Furthermore, LLDPE has a low elastic modulus, making expansion straightforward and it has great elongation, enabling stretching expansion for future prototypes. The HX was designed for crossflow because low pressure drop is required and high effectiveness is not required. The left image in Figure 1 shows the laser-welding pattern for the hot air flowing from right to left. The right image is the cold flow laser-welding pattern with flow going from top to bottom. These layers alternate, and the weld dot separation is 1 cm. When the patterns are superimposed, the dots do not overlap. The lines cross, creating a weld all the way down the EMHX, precluding expansion there.

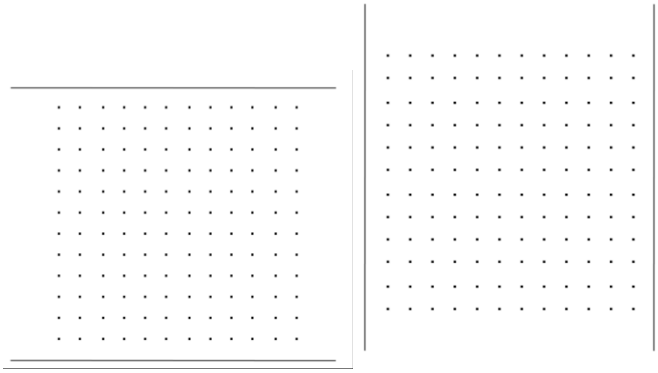

Figure 1 Alternating laser welding patterns.

The welds were made with an open-source polymer laser welding apparatus previously described [13]. It was difficult to achieve acceptable weld strength and only having the laser weld the top two layers together, but not the top three. Therefore, wood-fiber based blocking "fingers" were used to prevent the welding of the third layer. These fingers were inserted in one direction for one pattern, and rotated 90° for the opposite pattern (see Figure 1).

Then the weld strength was confirmed to be equivalent to the LLDPE material for short times with an ultimate strength of

~2000 N/cm^2. However, creep is a significant problem, so it is probably advisable to stay within 300 N/cm^2, especially at elevated temperatures. With 2 mm circular welds, and a weld separation of 1 cm, this could support a pressure of 0.1 atm. Operation is more like 0.0025 atmospheres (1 inch of water), which provides significant safety factor.

Figure 2 shows one expanded "pillow," one half of the final HX.

Figure 2 One expanded "pillow," one half of the final EMHX.

Each layer of the pillow was trimmed to the weld zone except for the top and bottom layers to be attached to the sub-manifolds.

Figure 3 shows three views of one of the sub-manifolds, which distributes the airflow from the small port to the many channels in the EMHX. The sub-manifolds, were designed in OpenSCAD and fabricated with an open-source RepRap 3-D printer [14] of the biopolymer polylactic acid (PLA). This allowed for custom shapes while maintaining the necessary mechanical strength [15]. The sub-manifolds were affixed to the HX pillows with permanent glue (E6000).

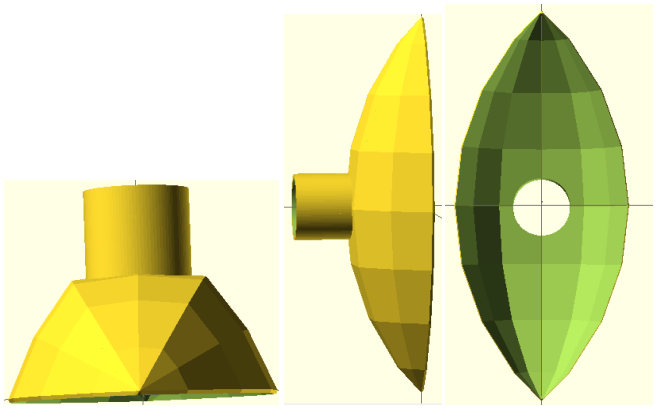

Figure 3 Computer aided drawing of manifold (three views).

The EMHX flattened out in a few seconds away from the manifolds after the inflation air was ceased. Therefore, a rigid frame designed as a cross to span between the four sub-manifolds was required to maintain expansion, which was attached to the LLDPE pillow with low-temperature hot-melt adhesive. Expansion was achieved with shop vacuum inflation.

For the prototypes, mechanical clips were placed over the corners to prevent air from circumventing from one flow path to another. The pressure applied by the clips was significantly greater than the expansion pressure, and far greater than operation pressure. Alternatively, a permanent method like bolts could be used.

Figure 4 shows the final assembled EMHX constructed with black ABS pipes with holes for each sub-manifold to form the "meta-manifolds" to distribute the flow to the individual pillows. To allow for variability in the positioning of the manifolds, flexible hose sections (shown in white) were used for connection to the meta-manifolds.

Figure 4 Assembled EMHX.

TESTING PROCEDURE

The equipment used for effectiveness testing was:

- 2 Delta Centrifugal Fans BFB1012H
- 12 Volt Power Supply
- Hot Air Gun
- 4 Omega Type K fine wire thermocouples

- Omega 8 channel data recorder
- Extech 4118 Digital Anemometer
- Dwyer Series 477 Digital Manometer

The manometer measured the pressure drop. The anemometer was used to determine the flow rate. The hot air gun supplied the air for one of the fans (see Figure 5). The other fan simply drew in room temperature air.

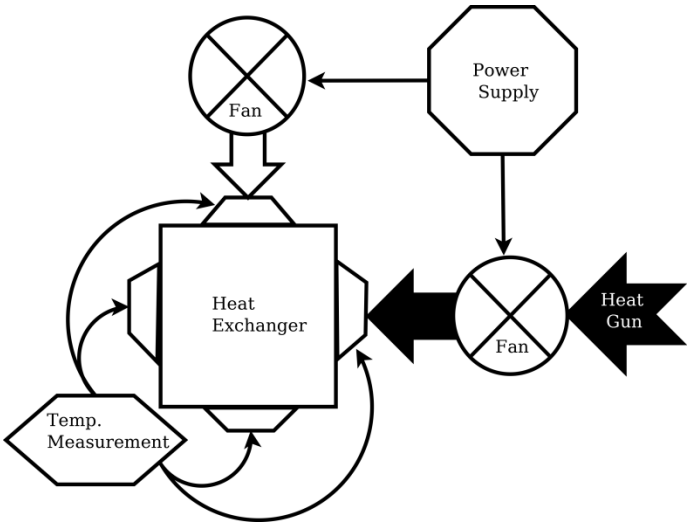

Figure 5 Effectiveness test setup.

RESULTS

The pressure drops are shown in Table 1. The hot effectiveness is how close to the hot flow approached the inlet cold temperature. Similarly, the cold effectiveness is how close the cold flow approached the inlet hot temperature. The hot and cold effectivenesses at maximum flow were 85% and 56%, respectively. The hot effectiveness is higher because the HX lost heat to the environment.

Table 1 HX performance parameters at maximum flow

Flow path	**Air-flow (L/s)**	**Air-flow (m^3/h)**	**Press-ure drop (Pa)**	**Effec-tive-ness**	**Heat trans-ferred (W)**	**Elec-trical power re-quired**
Hot	2.8		230	85%	25	7.1
Cold	4.0		160	56%	23	7.1

The average of the hot and cold effectivenesses were calculated for the prototype and the data are plotted in Figure 6. As expected, the effectiveness falls with increasing airflow.

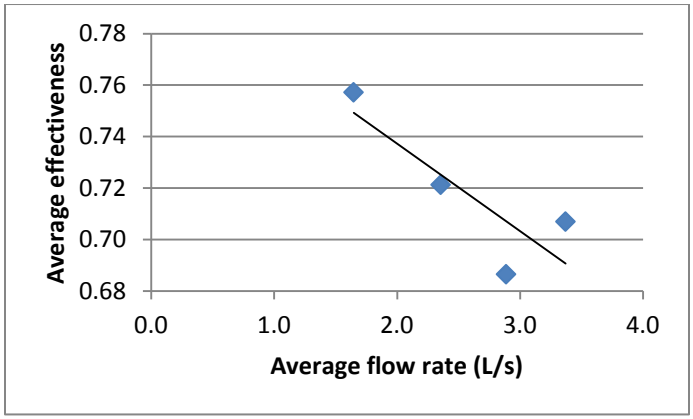

Figure 6 Effectiveness as a function of airflow.

DISCUSSION

Significant energy savings can be achieved by making ground vehicle heating, ventilating, and air conditioning (HVAC) systems more efficient. In light-duty vehicles, people typically use "max AC" to cool the car down, and "max AC" means recirculating about 85% of the air. However, when the cabin air is hotter than the outside air, it is less efficient to recirculate. Then people will typically take it off "max AC" when the car is cooled down, not recirculating, when it would actually be beneficial to recirculate. Therefore, an automatic system that senses when the cabin air is cooler than the outside and starts recirculation would save a large amount of energy used for vehicle HVAC. Furthermore, once the automatic system is implemented, more energy could be saved by activating an HRV HX on the fraction of the air that is not recirculated when the cabin air is cooler than outdoor air (see Figure 7).

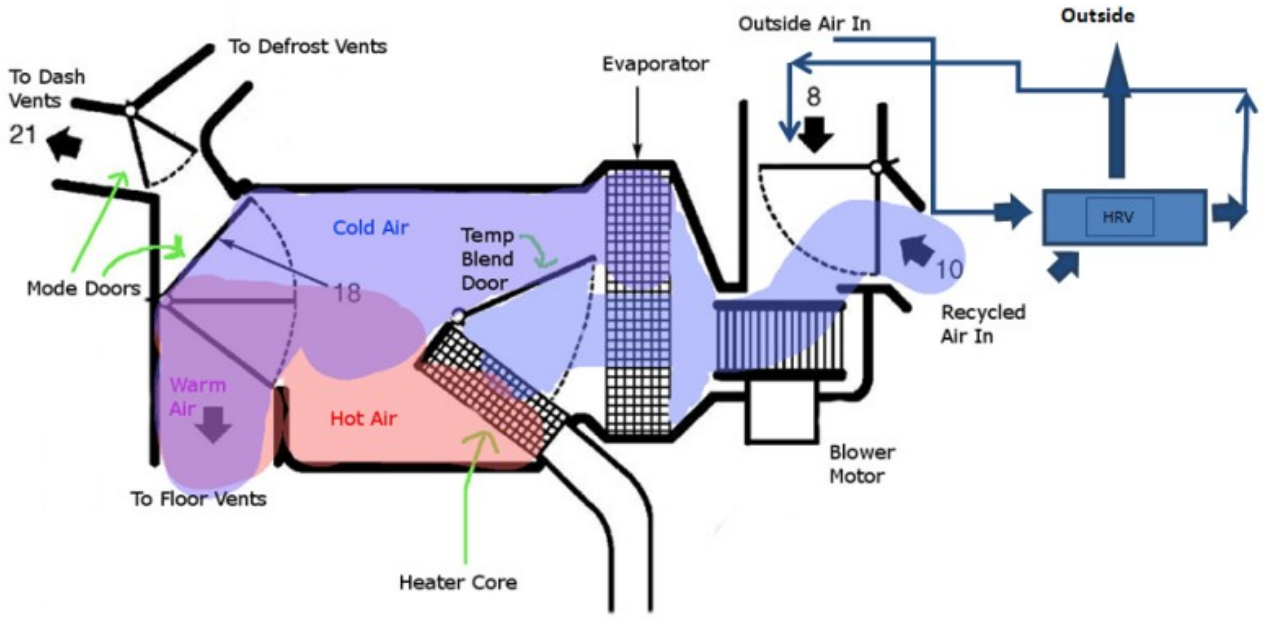

Figure 7 Vehicle HRV schematic.

Table 2 shows the assumptions required to estimate the energy savings. This analysis ignores pressure drop in the HX (not conservative) and ignores the weight and volume penalty of the HX (not conservative). However, it also assumes linear cooldown of the cabin (conservative because an exponential cooldown would spend more time when heat recovery makes sense), no stratification (conservative because drawing cooler air near the floor would make heat recovery more effective), and temperature economizing (conservative, as taking into account the humidity of the air (enthalpy economizing) would save more energy). Therefore, the overall result should be reasonable. The effectiveness value used is the curve fit at maximum flow because this is the most economical. The average effectiveness is used because temperature of the surroundings of the HRV are likely to be similar to the average temperature of the HRV (the average of cabin temperature and outdoor temperature).

Table 2 Air conditioning energy savings

General parameters	
Effectiveness	69%
Supply air temp (˚C)	7
Supply air humidity ratio (g H_2O/g air)	0.0065
Heat of vaporization (J/g)	2300
Cabin air temp (˚C)	24
Ventilation % when recirculating and cabin is cooled down	15%
Cooling required on recirculated air (˚C)	17
Non-humid case	
Ambient temperature (˚C)	32
% humidity	30%
Humidity ratio of ambient (g H_2O/g air)	0.012
Sensible equivalent cooling from humidity removal (˚C)	13
Sensible cooling of ambient (˚C)	25
HX cooling savings (˚C)	5.5
HX energy savings on ventilation air	15%
Ventilation air fraction of total load when cooled down	28%
HX energy savings when cabin is cooled down	4.1%
Humid case	
Ambient temperature (˚C)	29
% humidity	60%
Humidity ratio of ambient (g H_2O/g air)	0.016
Sensible equivalent cooling from humidity removal (˚C)	21
Sensible cooling (˚C)	22
HX cooling savings (˚C)	3.5
HX energy savings on ventilation air	8%
Ventilation air fraction of total load when cooled down	31%
HX energy savings when cabin is cooled down	2.5%

Table 3 shows that the fraction of air-conditioning energy savings is approximately 2%. Air-conditioning consumes approximately 6% of light-duty vehicle energy [16]. Since U.S. light-duty vehicles consume approximately 90 billion gallons of gasoline per year [17], the HRVs would save about 110 million gallons of gasoline per year. With the average gas price in the U.S. in 2013 of $3.58/gallon [18] the potential energy savings are ~$400 million/year.

Table 3 Overall energy savings

Overall U.S.	
% of AC load in humid areas	60%
Weighted average savings of HX of AC when cabin is cooled down	3.1%
% of AC energy when cabin is cooled down	60%
% of car AC energy use saved by HX	2.0%
% of car energy use saved by HX	0.12%

Additional savings could be achieved in buses, passenger trains, and medium and heavy-duty trucks. The economics would be even stronger in these applications because of the greater duty cycle. Furthermore, in light-duty vehicles that are plug-in hybrids or battery electric vehicles, for much or all of the time, there is not waste engine heat to heat the cabin. Even in conventional vehicles, in order to bring the cabin air temperature up to a comfortable temperature faster (before the engine is warmed up), the trend is towards auxiliary heating. In these cases, electric resistance or a heat pump must be used to provide heat, with considerable energy cost. The HRV would save energy in heating mode as well when the cabin air is greater temperature than outdoor air temperature, so the energy savings would be greater in these vehicles, and the economics would be more favorable than for other light-duty vehicles.

Air-conditioning systems are sized for the cool-down case when the car has soaked in the sun. Part of this cool-down time is when the cabin air is cooler than the outdoor air, so the HRV could reduce the size and weight of the air conditioning equipment. The better control system would also reduce the size and weight of the air-conditioning equipment. This may reduce the cost of the vehicle and have additional efficiency benefits, but these have been conservatively ignored in the present analysis.

The effectivenesses are not too high, but represent a large improvement considering that the competition is 0% because there are no air-to-air HXs used in vehicles today because of cost. In this study, a low-cost HX was demonstrated that was able to save about 2% of energy for the air-conditioning system. It is expected that the useful heat transferred is the heat removed from the hot airflow, because the HX is meant to cool down the air before it goes into the cold side of the air conditioner and then to the passenger compartment. However, the surroundings of the HRV are likely to be similar to the average temperature of the HRV (the average of cabin temperature and outdoor temperature), so the useful heat transferred would be the average of the heat transferred in the hot and the cold streams. This 28 W (adjusted for the average temperature difference encountered by the vehicle) is significantly greater than the electrical power of the fans, which sum to 14 W. When considering the power draw on the engine, it requires less mechanical energy to create a unit of cooling energy than to create a unit of electrical energy. However, the much larger fan required for the full vehicle HVAC system would be significantly more efficient than the fans used in the EMHX experiment. Therefore, despite the increased parasitic loss associated with moving air through the EMHX, the energetic contribution of the EMHX is highly net positive.

FUTURE WORK

Future work includes commercialization of this vehicle HRV application. Furthermore, many other applications would likely be appropriate for the EMHX. Early applications would be those that LLDPE could work for, i.e. low pressure and low temperature. These include building HRVs, indirect-direct evaporative cooling systems, power plant condensers, natural gas regasification, and cooling tower isolation HXs. Longer-term future work includes investigating composites, metals, and ceramic polymer precursors.

CONCLUSION

The EMHX shows promise for the application of vehicle HRVs. Though the channels in this prototype would not be considered micro, other methods of joining could be employed, like mask laser welding and inkjet printing of adhesives. These could indeed produce channels with < 1 mm hydraulic diameter. With the potential lower-cost of this type of HX made possible by mass production, other new applications could be made feasible. Furthermore, the EMHX could be applied to existing applications where metals or ceramics are required, just not those requiring extremely high pressure or disassembly for cleaning. The lower cost means that the optimal effectiveness is higher, opening up the possibility of tens of percent of primary energy savings.

ACKNOWLEDGEMENTS

Ray Radebaugh and Moncef Krarti provided valuable feedback. Jill Stone, Brennan Tymrak, Michael Poszywak, Paolo Clavijo, and Jeff DeCelles provided experimental assistance.

FUNDING

The New York State Energy Research and Development Authority provided funding for this project. The American Society of Heating, Refrigeration, and Air Conditioning Engineers Graduate Research Fellowship and the University of Colorado at Boulder Technology Transfer Office Proof of Concept Grant provided financial support for early development of the technology.

REFERENCES

[1] Zaheed, L. and Jachuck, R.J.J., Review of polymer compact heat exchangers, with special emphasis on a polymer film unit. *Applied Thermal Engineering*, vol. 24, num. 16, p. 2323-58, November 2004.

[2] Greenblatt, J.B., et al., Baseload wind energy: modeling the competition between gas turbines and compressed air energy storage for supplemental generation. *Energy Policy*, 2007, 35, p. 1474-1492.

[3] United Nations Development Programme, Human development report 2001: Making new technologies work for human development (Oxford: Oxford University Press, 2001), Available: http://hdr.undp.org/reports/global/2001/en/

[4] Denkenberger, D.C., Pearce, J.M., Compound parabolic concentrators for solar water heat pasteurization: numerical simulation. *Proceedings of the Solar Cookers International Conference*, July, Granada, Spain, 2006.
[5] Ganzevles, F.L.A., Drainage and condensate heat resistance in dropwise condensation of multicomponent mixtures in a plastic plate heat exchanger, PhD. Thesis, 2002, Technishe Universiteit Eindhoven.
[6] Hart, G.K., C-o Lee, and Latour, S.R., Development of plastic heat exchangers for ocean thermal energy conversion, 141 pages, A092503, Jan 1979.
[7] Greenbox http://www.greenbox.uk.com/ accessed April 1, 2008.
[8] Ogando, J., And now—an injection-molded heat exchanger. Design News Materials Editor, U.S. -- *Global Design News*, November 1, 2000.
[9] Ashman, S., Kandlikar, S., A review of manufacturing processes for microchannel heat exchanger fabrication, *Proceedings of the Fourth International Conference on Nanochannels, Microchannels and Minichannels*, June, Limerick, Ireland, 2006.
[10] Denkenberger, D.C., Brandemuehl, M.J., Pearce, J.M., and Zhai, J., Expanded microchannel heat exchanger: Design, fabrication, and preliminary experimental test, *Proceedings of the Institution of Mechanical Engineers, Part A: Journal of Power and Energy,* Vol 226, No. 4, June 2012.
[11] McQuiston, F.C., Parker, J.D., Spitler, J.D., Heating, ventilating, and air conditioning analysis and design, sixth edition. John Wiley & Sons, Inc. USA, 623 pages, 2005.
[12] Denkenberger, D.C., Microchannel expanded heat exchanger, U.S. Provisional Application No.: 13/513276, November 2012.
[13] Pearce, J.M., *Open-source lab: How to build your own hardware and reduce research costs*, Elsevier, 2014.
[14] Jones, R., Haufe, P., Sells, E., Iravani, P., Olliver, V., Palmer, C., & Bowyer, A., Reprap- the replicating rapid prototyper. Robotica, 29 (1), 177-191, 2011.
[15] Tymrak, B., Kreiger, M., Pearce, J.M., Mechanical properties of components fabricated with open-source 3-D printers under realistic environmental conditions, *Materials and Design* (in press, 2014).
[16] Johnson, V.H., Fuel Used for Vehicle Air Conditioning: A State-by-State Thermal Comfort-Based Approach, national renewable energy laboratory, 2002-01-1957.
[17] Davis, S.C., Diegel, S.W., and Boundy, R.G., Transportation energy data book: Edition 32, Oak Ridge National Laboratory for U.S. Department of Energy, 2013.
[18] U.S. Energy Information Agency, Petroleum and Other Liquids, Annual Price Data, 2013.